Bull. Korean Fish. Soc. 25(6), 443~456, 1992

韓水誌, 25(6), 443~456, 1992

Coastally Trapped Waves over a Double Shelf Topography(II): Free Waves with Linear Topographies

Ig-Chan PANG
Department of Oceanography, National University of Cheju, Cheju 690-120, Korea

For a linear double shelf bottom topography as in the Yellow Sea, the dispersion relation of coastally trapped waves is derived for the general case including high-frequency and short waves and for the case of low-frequency and long waves. With linear bottom topography, the governing equation is Bessel's equation for the latter case but Kummer's equation for the former case. Hypergeometric Functions, which are the solutions of Kummer's equation, are derived and converted to various special functions for the limiting cases.

On a double shelf topography, the divergence effects of horizontal flow are important for the wave dynamics, irrespective of cross-shelf dimensions, while on a single shelf they are usually neglected when the cross-shelf dimension is much smaller than the Rossby deformation radius. The divergence effect allows the existence of Kelvin wave and reduces the phase speeds of continental shelf waves. Finally, the frictionless eigenfunctions are proved to be orthogonal.

Introduction

The theories of coastally trapped waves have gradually been established and now there is little doubt about that coastally trapped waves play an important role in the coastal ocean response to applied wind stresses. The theories have been first developed for the single shelf case(Buchwald and Adams, 1968; Gill and Schumann, 1974; Huthnance, 1975, 1978; Brink and Allen, 1978; LeBlond and Mysak, 1978; Clarke and VanGorder, 1986; etc.) and thereafter for the various cases of different shelf such as submarine banks and trenches (Louis, 1978; Mysak etc., 1979, 1980, 1981; Brink, 1983). Recently, the theory for the double shelf case has been reported. Hsueh and Pang(1989) have developed the theory and shown a good assesment of its application to the Yellow Sea. Pang (1991) has shown the general properties of coastally trapped waves over an exponential double shelf topography. An exponential topography allows analytical solutions in the whole ranges of wave number for non-divergence case. Over a double shelf topography, two sets of waves propagate in opposite directions, with the shallow waters to the right in the northern hemisphere. The group velocities of shelf waves have the same direction as the phase velocities in the long waves, but the opposite direction in the short waves.

An exponential topography, however, does not allow analytical solution for divergence case. The horizontal flow divergence is essential for explaining a major part of the ocean response on a double shelf(Hsueh & Pang, 1989), while it is ignored on a single shelf when the cross-shelf dimension is much smaller than Rossby deformation radius. Analytical solutions for divergence case could be obtained by a linear topography. Hsueh & Pang

* This research is supported by Korea Science Foundation(한국과학재단) Grant 893-0505-006-2, 1989~1991.

(1989) have obtained them for long waves. However, in spite of the basic establishment, the theory should be further developed to include short waves and the prove the orthogonality of the bases. The purpose of this paper is to develop the theory of coastally trapped free waves over a double shelf topography for divergence cases. It is extended to short waves, which is necessary for small scale coastal ocean dynamics such as reflecting or scattering, and the orthogonality is proved for eigenfunction expansions.

Field Equation and Boundary conditions

Small perturbations to a barotropic ocean satisfy the equation:

$$HP_{xxt}+H_xp_{xt}+Hp_{yyt}+fH_xp_y+(rp_x)_x-\frac{f^2-\omega^2}{g}p_t=-\frac{f^2-\omega^2}{g}p_{at}+f(Y_x-X_y) \quad (1)$$

In this equation, x, y, t, p, g, f, r, H, p_a, X and Y refer respectively to cross-shelf distance(eastward positive), alongshore distance(northward positive), time, perturbation pressure divided by mean water density, acceleration due to gravity, Coriolis parameter, bottom resistance coefficient, water depth, atmospheric perturbation pressure divided by mean water density, kinematic stresses in x and y direction at surface(the wind stresses divided by mean water density). Subscripts indicate derivatives.

We have chosen the Yellow Sea to examine a double shelf system. Fig. 1 shows the bottom topography of the Yellow Sea and the bathymetric transects used for some illustrating calculations. A simple approximation to the depth profile of the double shelf is shown in Fig. 2.

Fig. 2 shows a schematic representation of the coordinates system and geometry of two shelves of linear depth profile and a level intervening region. To begin with, an intervening region is put between the two shelves so that shelf 1, intervening region, and shelf 2 are placed in $-B_1\le x\le$, $0\le x\le L_m$, and $L_m\le x\le B_2$, respectively. So, the linear bottom

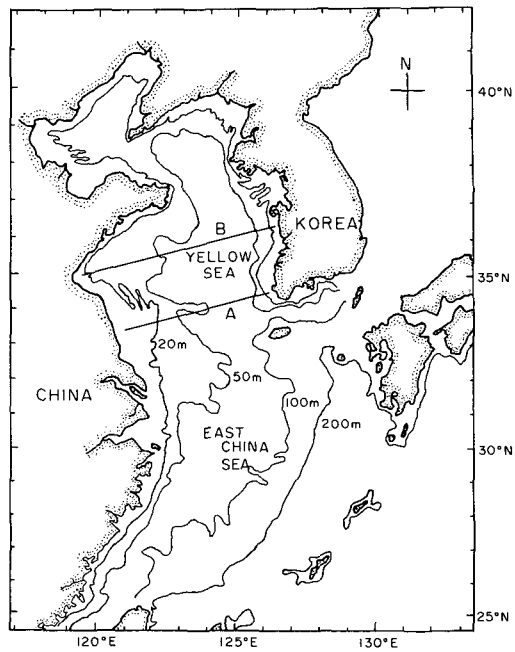

Fig. 1. Map of the Yellow Sea. Sections labled A and B are those along which depth profiles are taken.

topography (H) can be set as follows:

$$H(x)=\begin{cases} H_1=H_0\dfrac{x+L_1}{L_1} & -L_1\le x\le 0 \\ & \text{in shelf 1} \\ H_m=H_0 & 0\le x\le L_m \\ & \text{in middle area} \\ H_2=-H_0\dfrac{x-L_2}{L_2-L_m} & L_m\le x\le L_2 \\ & \text{in shelf 2} \end{cases} \quad (2)$$

At the coastal boundaries, the no-flux boundary condition is applied, which means that the depth integrated offshore velocity vanishes. For most cases of coastal ocean dynamics, wind stresses are applied through the coastal boundary condition. Near coast, the Ekman flux produced by alongshore wind stress gives rise to the convergence and divergence fluxes, which drive the interior flow. Consequently, the interior flows are driven by the wind stress applied through the coastal boundary condition. In the case of a linear depth profile, Mitchum and Clarke(1986) have concluded that the place where the water depth is about 3 times

the Ekman layer thickness is the best place for the imposition of the no-flux condition. At x=0, L_m, the 'continuous pressure' and the 'continuous transverse velocity' boundary conditions are applied, as follows:

$$P_{1xt}+\frac{r}{h}P_{1x}+fP_{1y}=f\frac{Y}{h} \quad \text{at } x=-B_1 \qquad (3\text{-}1)$$

$$P_1=P_m, \quad \text{at } x=0 \qquad (3\text{-}2)$$

$$P_{1xt}+fP_{1y}=P_{mxt}+fP_{my}, \quad \text{at } x=0 \qquad (3\text{-}3)$$

$$P_m=P_2, \quad \text{at } x=L_m \qquad (3\text{-}4)$$

$$P_{mxt}+fP_{my}=P_{2xt}+fP_{2y}, \quad \text{at } x=L_m \qquad (3\text{-}5)$$

$$P_{2xt}+\frac{r}{h}p_{2x}+fP_{2y}=f\frac{Y}{h} \quad \text{at } x=B_2 \qquad (3\text{-}6)$$

To solve the above eigenvalue problem, either frictionless eigenfunction or frictional eigenfunction can be used. Frictionless eigenfunction has been used conventionally, but Webster(1985) has started to use frictional eigenfunction. In this work, frictionless eigenfunction is used.

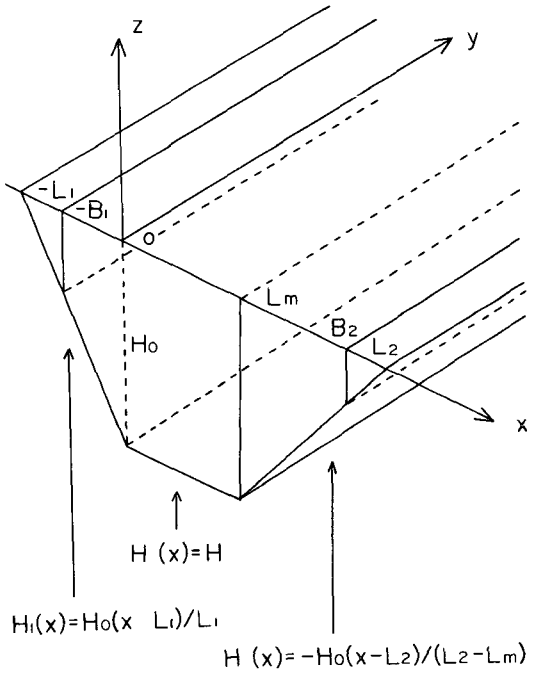

Fig. 2. Schematic representation of the coordinate system and geometry of two shelves of linear depth profile and a level intervening region. The coordinates x, y, and z refer to the cross-shelf, alongshore, and vertical directions and are oriented eastward, northward, and upward, respectively.

Dispersion Relations

1. General Case including High-frequency and Short-waves

The field equation (1) yields for divergent and inviscid free waves

$$Hp_{xxt}+H_xp_{xt}+Hp_{yyt}+fH_xp_y-\frac{f^2-\omega^2}{g}pt=0 \qquad (4)$$

Upon substituting for the pressure, $p=F(x)\phi(y+ct)$, (4) yields

$$(HF')'-\ell^2HF+\frac{f}{c}H'F+\frac{\omega^2-f^2}{g}F=0 \qquad (5)$$

where the 'prime' means the derivative with respective to x, and ℓ, ω, and c are, respectively, wave number, frequency, and phase speed, such that $c=\frac{\omega}{\ell}$. Equation (5) with the depth profiles given by (2) yields the following eigen value problem for the frictionless eigenfunction F(x):

$$[\alpha(x+L_1)F_1']'+(-\ell^2x+\frac{f}{c}+\frac{\omega^2-f^2}{g\alpha})F_1=0$$
$$-L_1\le x\le 0 \qquad (6\text{-}1)$$

$$F_m''+[-\ell^2+\frac{\omega^2-f^2}{gH_0}]F_m=0$$
$$0\le x\le L_m \qquad (6\text{-}2)$$

$$[\beta(x-L_2)F_2']'+(-\ell^2x+\frac{f}{c}+\frac{\omega^2-f^2}{g\beta})F_2=0$$
$$L_m\le x\le L_2 \qquad (6\text{-}3)$$

finite condition at $x=-L_1$ (7-1)

$F_1=F_2$ at $x=0$ (7-2)

$F_1'=F_m'$ at $x=0$ (7-3)

$F_m=F_2$ at $x=L_m$ (7-4)

$F_m'=F_2'$ at $x=L_m$ (7-5)

finite condition at $x=L_2$ (7-6)

F_1, F_m and F_2 represent the eigenfunctions over, respectively, the shelf 1, intervening region, and shelf 2. α and β are the slope coefficients of shelf 1 and shelf 2, respectively.

The solutions of (6) are

$$F_1=C\exp[-|\ell|(x+L_1)]$$
$$M[a_1,1,2|\ell|(x+L_1)]$$
$$-L_1<x<0 \qquad (8\text{-}1)$$

$$F_m = A\exp(mx) + B\exp(-mx) \quad 0<x<L_m \tag{8-2}$$

$$F_2 = D\exp[\,|\ell|\,(x-L_2)\,]\,M[a_2,1,2\,|\ell|\,(L_2-x)] \quad L_m<x<L_2 \tag{8-3}$$

where M is the confluent hypergeometric function M(a,b,x). A, B, C, and D are arbitrary constants, and a_1, a_2 and m are given by

$$a_1 = 1/2 - \frac{\ell}{2\,|\ell|\,\omega} - \frac{\omega^2-f^2}{2g\,|\ell|\,\alpha}$$

$$a_2 = 1/2 + \frac{\ell}{2\,|\ell|\,\omega} + \frac{\omega^2-f^2}{2g\,|\ell|\,\beta}$$

$$m = \left(\ell^2 - \frac{\omega^2-f^2}{gH_0}\right)^{1/2}$$

There are two confluent hypergeometric functions M(a,b,x), U(a,b,x) to satisfy Kummer's equation. The finite boundary condition get rid of U(a,b,x) which has a singularity at x=0. The dispersion relation is

$$\tanh(mL_2)([\,|\ell|^2+m^2]M_1M_3 - 2\,|\ell|^2 a_3M_1M_4 - 2\,|\ell|^2 a_1M_2M_3 + 4\,|\ell|^2 a_1a_3M_2M_4) - 2\,|\ell|\,m(M_1M_3 - a_3M_1M_4 - a_1M_2M_3) = 0 \tag{9}$$

where $M_1 = M(a_1,1,2\,|\ell|\,L_1)$,
$M_2 = M(a_1+1,2,2\,|\ell|\,L_1)$,
$M_3 = M(a_3,1,2\,|\ell|\,[L_2-L_m])$,
$M_4 = M(a_3+1,2,2\,|\ell|\,[L_2-L_m])$.

When L_m goes to infinity as shown in Fig. 4(a), the dispersion relation (9) reduces to

$$([\,|\ell| - m]M_1 - 2\,|\ell|\,a_1M_2)\cdot([\,|\ell| - m]M_3 - |\ell|\,a_3M_4) = 0 \tag{10}$$

which yields two independent sets of waves as follows:

$$M_1/M_{1x} = \frac{|\ell|}{L_1(\,|\ell| - m)} \quad \text{or}$$

$$M_3/M_{3x} = \frac{|\ell|}{(L_2-L_m)(\,|\ell| - m)} \tag{11}$$

since $M_{1x} = 2L_1a_1M_2$ and $M_{3x} = 2(L_2-L_m)a_3M_4$. For non-trivial solutions, a_1 and a_3 must be negative, which give the positive and negative phase speeds, respectively.

When L_m goes to zero(double shelf case) as shown in Fig. 4(b), it yields

$$M_1M_3 - a_3M_1M_4 - a_1M_2M_3 = 0 \tag{12}$$

This can be changed as $1 - a_3\frac{M_4}{M_3} = a_1\frac{M_2}{M_1} \equiv p$, therefore,

$$\frac{M_1}{M_{1x}} = \frac{p_1}{2L_1} \quad \text{if } a_1<0,\ a_3>0 \tag{13-1}$$

$$\frac{M_3}{M_{3x}} = \frac{p_2}{2(L_2-L_m)(p_2-1)} \quad \text{if } a_1>0,\ a_3<0 \tag{13-2}$$

where $p_1 = 1 - a_3\frac{M_4}{M_3}$ and $p_2 = a_1\frac{M_2}{M_1}$. They are dependent on the both shelves through p.

In this case the dispersion relation (9), (10), (13) include Kelvin waves, continental shelf waves, and Poincare waves. Confluent hypergeometric function is converted to various different functions, such as Bessel Function, for some limiting cases. It could cover theoretically whole ranges of coastally trapped waves. However, confluent hypergeometric function has not been fully developed so that it is not practical yet to use (9). Mostly, we are looking at the case of low-frequency and long waves. The dispersion relation for the limiting case will be derived additionally in the next section. Therefore, the above results only show a possibility to expand the theory of coastally trapped waves to the general case in the future. Presently, the shelf wave theory for low-frequency and long-wave case, which is shown in the next section, is needed.

2. Low-frequency and Long Wave Case

The usual low-frequency and long-wave approximation will be invoked in this section. The field equation (1) yields for divergent, inviscid, low-frequency, long free waves

$$(Hp_{xt})_x + fH_xP_y - \frac{f^2}{g}pt = 0 \tag{14}$$

Upon substituting for the pressure, $p = F(x)\phi(y+ct)$, (14) yields

$$(HF')' + \frac{f}{c}H'F - \frac{f^2}{g}F = 0 \tag{15}$$

where the 'prime' means the derivative with respective to x and c is the phase speed. Equation

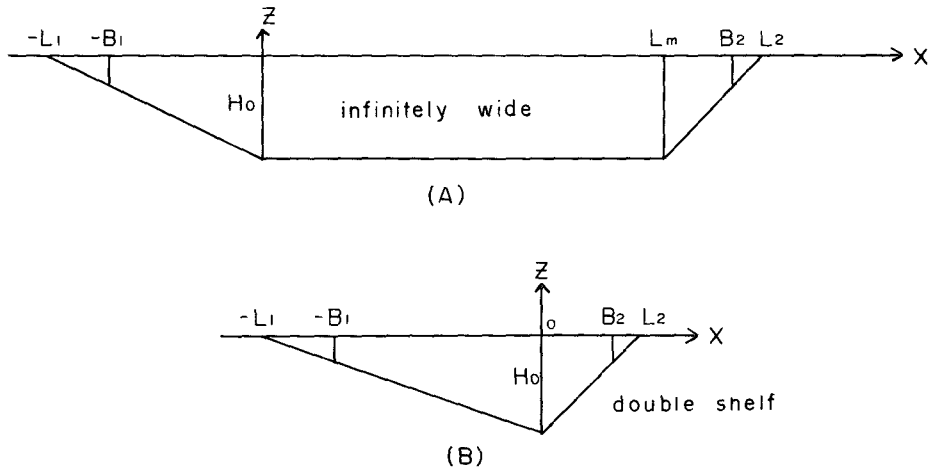

Fig. 3. Schematic representations of the cross-shelf sections for (A) two shelves with an infinitely wide intervening region, and (B) a double shelf (two adjoining shelves).

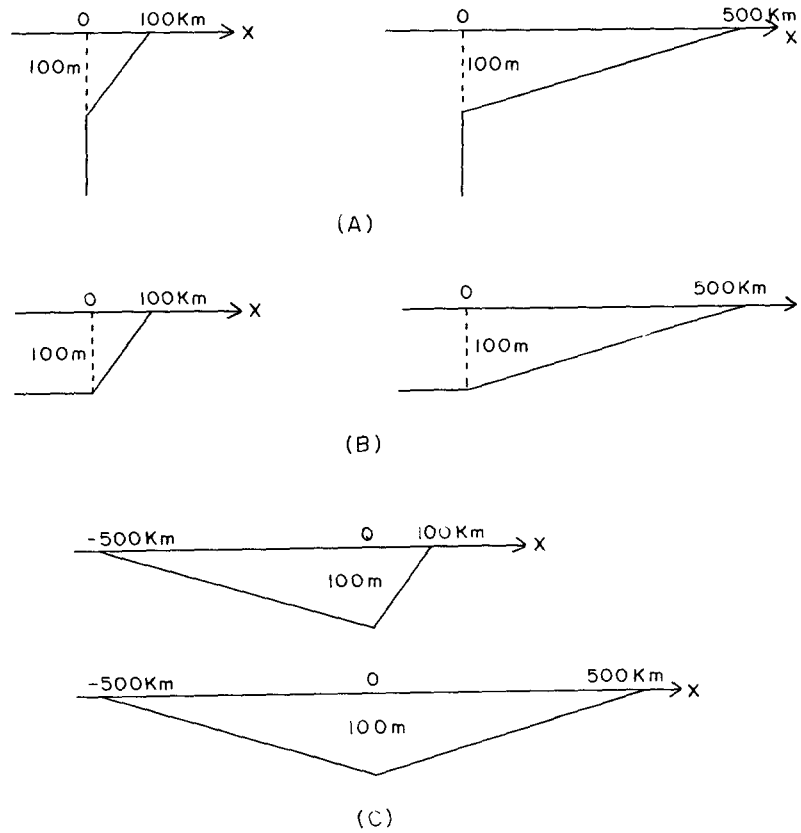

Fig. 4. Schematic representations of the cross-shelf for (A) a single shelf adjacent to an infinitely deep water region, (B) a single shelf adjacent to a region of the finite depth equal to the greatest depth of shelf, and (C) a double shelf. The greatest depth of shelf are 100*m* for all cases and the shelf widths are 100*m* and 500*m* in each case.

(15) with the depth profiles given by (2) yields the following eigen value problem for the frictionless eigenfunction F(x):

$$[\alpha(x+L_1)F_1']'+\mu_1F_1=0 \qquad -L_1\le x\le 0 \qquad (16\text{-}1)$$
$$F_m''-\lambda^2F_m=0 \qquad 0\le x\le L_m \qquad (16\text{-}2)$$
$$[\beta(x-L^2)F_2']'+\mu_2F_2=0 \qquad L_m\le x\le L_2 \qquad (16\text{-}3)$$

$$F_1'+\frac{f}{c}F_1=0 \qquad \text{at } x=-B_1 \qquad (17\text{-}1)$$
$$F_1=F_m \qquad \text{at } x=0 \qquad (17\text{-}2)$$
$$F_1'=F_m' \qquad \text{at } x=0 \qquad (17\text{-}3)$$
$$F_m=F_2 \qquad \text{at } x=L_m \qquad (17\text{-}4)$$
$$F_m'=F_2' \qquad \text{at } x=L_m \qquad (17\text{-}5)$$
$$F_2'+\frac{f}{c}F_2=0 \qquad \text{at } x=B_2 \qquad (17\text{-}6)$$

where $\mu_1=\frac{f}{c}-\frac{f^2}{g\alpha}$, $\mu_2=\frac{f}{c}-\frac{f^2}{g\beta}$,

$$\lambda^2=\frac{f^2}{gH_0}, \quad \alpha=\frac{H_0}{L_1}, \quad \beta=-\frac{H_0}{L_2-L_m}.$$

Here, F_1, F_m and F_2 represent the eigenfunctions over, respectively, the shelf 1, intervening region, and shelf 2. λ is the reciprocal of barotropic deformation radius, and α and β are the slope coefficients of the shelves 1 and shelf 2, respectively.

The solution of the above eigenvalue problem leads to a dispersion relation that allows the determination of phase speed c, as follows:

$$\exp(-m_1L_2)\frac{J_0(2b_1)J_0(2b_2)}{J_0(2a_1)J_0(2a_2)}\left[\frac{f}{c}-\frac{\mu_1}{b_1}\frac{J_1(2b_1)}{J_0(2b_1)}\right]\cdot\left[\frac{f}{c}-\frac{\mu_2}{b_2}\frac{J_1(2b_2)}{J_0(2b_2)}\right]\cdot\left[\lambda+\frac{\mu_1}{a_1}\frac{Y_1(2a_1)}{Y_0(2a_1)}\right]\cdot\left[\lambda-\frac{\mu_2}{a_2}\frac{Y_1(2a_2)}{Y_0(2a_2)}\right]$$

$$-\exp(-m_1L_2)\frac{J_0(2b_1)Y_0(2b_2)}{J_0(2a_1)Y_0(2a_2)}\left[\frac{f}{c}-\frac{\mu_1}{b_1}\frac{J_1(2b_1)}{J_0(2b_1)}\right]\cdot\left[\frac{f}{c}-\frac{\mu_2}{b_2}\frac{Y_1(2b_2)}{Y_0(2b_2)}\right]\cdot\left[\lambda+\frac{\mu_1}{a_1}\frac{Y_1(2a_1)}{Y_0(2a_1)}\right]\cdot\left[\lambda-\frac{\mu_2}{a_2}\frac{J_1(2a_2)}{J_0(2a_2)}\right]$$

$$-\exp(-m_1L_2)\frac{Y_0(2b_1)J_0(2b_2)}{Y_0(2a_1)J_0(2a_2)}\left[\frac{f}{c}-\frac{\mu_1}{b_1}\frac{Y_1(2b_1)}{Y_0(2b_1)}\right]\cdot\left[\frac{f}{c}-\frac{\mu_2}{b_2}\frac{J_1(2b_2)}{J_0(2b_2)}\right]\cdot\left[\lambda+\frac{\mu_1}{a_1}\frac{J_1(2a_1)}{J_0(2a_1)}\right]\cdot\left[\lambda-\frac{\mu_2}{a_2}\frac{Y_1(2a_2)}{Y_0(2a_2)}\right]$$

$$+\exp(-m_1L_2)\frac{Y_0(2b_1)Y_0(2b_2)}{Y_0(2a_1)Y_0(2a_2)}\left[\frac{f}{c}-\frac{\mu_1}{b_1}\frac{Y_1(2b_1)}{Y_0(2b_1)}\right]\cdot\left[\frac{f}{c}-\frac{\mu_2}{b_2}\frac{J_1(2b_2)}{J_0(2b_2)}\right]\cdot\left[\lambda+\frac{\mu_1}{a_1}\frac{J_1(2a_1)}{J_0(2a_1)}\right]\cdot\left[\lambda-\frac{\mu_2}{a_2}\frac{J_1(2a_2)}{J_0(2a_2)}\right]$$

$$-\exp(m_1L_2)\frac{J_0(2b_1)J_0(2b_2)}{J_0(2a_1)J_0(2a_2)}\left[\frac{f}{c}-\frac{\mu_1}{b_1}\frac{J_1(2b_1)}{J_0(2b_1)}\right]\cdot\left[\frac{f}{c}-\frac{\mu_2}{b_2}\frac{J_1(2b_2)}{J_0(2b_2)}\right]\cdot\left[\lambda-\frac{\mu_1}{a_1}\frac{Y_1(2a_1)}{Y_0(2a_1)}\right]\cdot\left[\lambda+\frac{\mu_2}{a_2}\frac{Y_1(2a_2)}{Y_0(2a_2)}\right]$$

$$+\exp(m_1L_2)\frac{J_0(2b_1)Y_0(2b_2)}{J_0(2a_1)Y_0(2a_2)}\left[\frac{f}{c}-\frac{\mu_1}{b_1}\frac{J_1(2b_1)}{J_0(2b_1)}\right]\cdot\left[\frac{f}{c}-\frac{\mu_2}{b_2}\frac{Y_1(2b_2)}{Y_0(2b_2)}\right]\cdot\left[\lambda-\frac{\mu_1}{a_1}\frac{Y_1(2a_1)}{Y_0(2a_1)}\right]\cdot\left[\lambda+\frac{\mu_2}{a_2}\frac{J_1(2a_2)}{J_0(2a_2)}\right]$$

$$+\exp(m_1L_2)\frac{Y_0(2b_1)J_0(2b_2)}{Y_0(2a_1)J_0(2a_2)}\left[\frac{f}{c}-\frac{\mu_1}{b_1}\frac{Y_1(2b_1)}{Y_0(2b_1)}\right]\cdot\left[\frac{f}{c}-\frac{\mu_2}{b_2}\frac{J_1(2b_2)}{J_0(2b_2)}\right]\cdot\left[\lambda-\frac{\mu_1}{a_1}\frac{J_1(2a_1)}{J_0(2a_1)}\right]\cdot\left[\lambda+\frac{\mu_2}{a_2}\frac{Y_1(2a_2)}{Y_0(2a_2)}\right]$$

$$-\exp(m_1L_2)\frac{Y_0(2b_1)Y_0(2b_2)}{Y_0(2a_1)Y_0(2a_2)}\left[\frac{f}{c}-\frac{\mu_1}{b_1}\frac{Y_1(2b_1)}{Y_0(2b_1)}\right]\cdot\left[\frac{f}{c}-\frac{\mu_2}{b_2}\frac{Y_1(2b_2)}{Y_0(2b_2)}\right]\cdot\left[\lambda-\frac{\mu_1}{a_1}\frac{J_1(2a_1)}{J_0(2a_1)}\right]\cdot\left[\lambda+\frac{\mu_2}{a_2}\frac{J_1(2a_2)}{J_0(2a_2)}\right]=0 \qquad (18)$$

where $a_1=(\mu_1L_1)^{1/2}$, $a_2=(-\mu_2[L_2-L_m])^{1/2}$, $b_1=(\mu_1[-B_1+L_1)^{1/2}$, $b_2=(\mu_2[B_2-L_3])^{1/2}$, and J_m and Y_m refer to the mth order Bessel Functions of the 1st and 2nd kind, and λ, μ_1, μ_2 are given above.

When L_m goes to infinity as shown in Fig. 3(a), the dispersion relation (18) reduces to

$$\left[\frac{J_0(2b_1)}{J_0(2a_1)}\left[\frac{f}{c}-\frac{\mu_1}{b_1}\frac{J_1(2b_1)}{J_0(2b_1)}\right]\cdot\left[\lambda-\frac{\mu_1}{a_1}\frac{Y_1(2a_1)}{Y_0(2a_1)}\right]-\frac{Y_0(2b_1)}{Y_0(2a_1)}\right.$$

$$\left[\frac{f}{c}-\frac{\mu_1}{b_1}\frac{Y_1(2b_1)}{Y_0(2b_1)}\right]\cdot\left[\lambda-\frac{\mu_1}{a_1}\frac{J_1(2a_1)}{J_0(2a_1)}\right]\Bigg]$$
$$\times\Bigg[\frac{J_0(2b_2)}{J_0(2a_2)}\left[\frac{f}{c}-\frac{\mu_2}{b_2}\frac{J_1(2b_2)}{J_0(2b_2)}\right]\cdot$$
$$\left[\lambda-\frac{\mu_2}{a_2}\frac{Y_1(2a_2)}{Y_0(2a_2)}\right]-\frac{Y_0(2b_2)}{Y_0(2a_2)}$$
$$\left[\frac{f}{c}-\frac{\mu_2}{b_2}\frac{Y_1(2b_2)}{Y_0(2b_2)}\right]\cdot\left[\lambda-\frac{\mu_2}{a_2}\frac{J_1(2a_2)}{J_0(2a_2)}\right]\Bigg]=0 \quad (19)$$

This shows two independent sets of coastally trapped wave, which means that if the shelves are apart sufficiently enough, two sets of coastally trapped waves do not interact with each other, as for an exponential topography (Pang, 1991).

When L_m goes to zero(double shelf case) as shown in Fig. 3(b), it yields

$$a_1\mu_2J_0(2b_1)J_0(2b_2)Y_0(2a_1)Y_1(2a_2)$$
$$\left[\frac{f}{c}-\frac{\mu_1}{b_1}\frac{J_1(2b_1)}{J_0(2b_1)}\right]\left[\frac{f}{c}-\frac{\mu_2}{b_2}\frac{J_1(2b_2)}{J_0(2b_2)}\right]$$
$$-a_1\mu_2J_0(2b_1)Y_0(2b_2)Y_0(2a_1)J_1(2a_2)$$
$$\left[\frac{f}{c}-\frac{\mu_1}{b_1}\frac{J_1(2b_1)}{J_0(2b_1)}\right]\left[\frac{f}{c}-\frac{\mu_2}{b_2}\frac{Y_1(2b_2)}{Y_0(2b_2)}\right]$$
$$-a_1\mu_2Y_0(2b_1)J_0(2b_2)J_0(2a_1)Y_1(2a_2)$$
$$\left[\frac{f}{c}-\frac{\mu_1}{b_1}\frac{Y_1(2b_1)}{Y_0(2b_1)}\right]\left[\frac{f}{c}-\frac{\mu_2}{b_2}\frac{J_1(2b_2)}{J_0(2b_2)}\right]$$
$$+a_1\mu_2Y_0(2b_1)Y_0(2b_2)J_0(2a_1)J_1(2a_2)$$
$$\left[\frac{f}{c}-\frac{\mu_1}{b_1}\frac{Y_1(2b_1)}{Y_0(2b_1)}\right]\left[\frac{f}{c}-\frac{\mu_2}{b_2}\frac{Y_1(2b_2)}{Y_0(2b_2)}\right]$$
$$-a_2\mu_1J_0(2b_1)J_0(2b_2)Y_1(2a_1)Y_0(2a_2)$$
$$\left[\frac{f}{c}-\frac{\mu_1}{b_1}\frac{J_1(2b_1)}{J_0(2b_1)}\right]\left[\frac{f}{c}-\frac{\mu_2}{b_2}\frac{J_1(2b_2)}{J_0(2b_2)}\right]$$
$$+a_2\mu_1J_0(2b_1)Y_0(2b_2)Y_1(2a_1)J_0(2a_2)$$
$$\left[\frac{f}{c}-\frac{\mu_1}{b_1}\frac{J_1(2b_1)}{J_0(2b_1)}\right]\left[\frac{f}{c}-\frac{\mu_2}{b_2}\frac{Y_1(2b_2)}{Y_0(2b_2)}\right]$$
$$+a_2\mu_1Y_0(2b_1)J_0(2b_2)J_1(2a_1)Y_0(2a_2)$$
$$\left[\frac{f}{c}-\frac{\mu_1}{b_1}\frac{Y_1(2b_1)}{Y_0(2b_1)}\right]\left[\frac{f}{c}-\frac{\mu_2}{b_2}\frac{J_1(2b_2)}{J_0(2b_2)}\right]$$
$$-a_2\mu_1Y_0(2b_1)Y_0(2b_2)J_1(2a_1)J_0(2a_2)$$
$$\left[\frac{f}{c}-\frac{\mu_1}{b_1}\frac{Y_1(2b_1)}{Y_0(2b_1)}\right]\left[\frac{f}{c}-\frac{\mu_2}{b_2}\frac{Y_1(2b_2)}{Y_0(2b_2)}\right]$$
$$=0 \quad (20)$$

The dispersion relation implies that the two sets of wave are dependent on each other if two shelves are close while they become independent single shelf waves if two shelves are separated far enough. The phase speeds c of two sets of waves is $g\alpha/f>c>0$ and $g\beta/f<c<0$, respectively. For the range of $g\alpha/f>c>0$, the set of waves propagate southward, while for the range $g\beta/f<c<0$, the set of waves propagate northward.

The dispersion relation looks complicated but its essential characteristics are the same as for a non-divergent case(Pang, 1991), except the 1st modes. The(exponential or linear) bottom shape itself does not make any basic difference. It should be noted that a linear topography is adapted in this paper for analytic solutions to a divergent case. In the divergence case, the phase speed of first modes shows different characteristics from that of the rest modes. It is comparable to the phase speed of gravity waves.

Table 1 shows phase speeds for 3 different cases of bottom topography: (A) a single shelf adjacent to an infinitely deep water region, (B) a single shelf adjacent to a region of the finite depth equal to the greatest depth of shelf, and (C) a double shelf. The greatest depth of shelf are 100*m* for all cases and the cases (A) and (C) have 2 sub-cases: a non-divergence case and a divergence case. The case (B) does not include a non-divergent case, since the divergence effect is essential to allow sea level fluctuations at the edge of shelf. Fig. 4 shows schematic representations of the cross-shelf bottom topography for the cases. From table 1, we can see 2 divergence effects.

One is for the 1st modes. For non-divergence cases, the phase speeds of the 1st modes are propotional to shelf width, which is a characteristics of continental shelf waves. However, for divergence cases, the phase speeds of the 1st modes vary inversely with shelf width. It is a characteristics of Kelvin wave. The phase speed of Kelvin wave over sloping bottom increases by steeper slope, which corresponds to narrow shelf width.(It should be noted that the 1st mode in the case (a) show both characteristics of Kelvin wave and continental shelf wave, because Kelvin wave is not allowed in the infinitely deep water.) It is the reason why sea level propagation is faster along the western coasts of Korean Peninsula than along the eastern coasts of China in the numerical model run for the 1980/81 winter(Hsueh and Romea, 1983). The other is

Table 1. The phase speeds of wave modes in the case of (a) a single shelf adjacent to an infinitely deep water region, (b) a single shelf adjacent to a region of finite depth equal to the greatest depth of the shelf, and (c) a double shelf. The greatest shelf water depths are 100*m* for all cases.

case	shelf width (in *km*)		phase speeds (*m/sec*) of first 3 modes					
			1	2	3	-1	-2	-3
A	100	non-divergent	6.16	1.17	0.48	-	-	-
		divergent	5.83	1.16	0.47	-	-	-
	500	non-divergent	30.78	5.84	2.38	-	-	-
		divergent	12.84	4.62	2.15	-	-	-
B	100	divergent	27.10	2.21	0.70	-	-	-
	500	divergent	15.90	6.41	2.84	-	-	-
C	500~100	non-divergent	7.29	2.68	1.38	-1.97	-0.64	-0.31
		divergent	14.70	5.31	2.37	-24.18	-1.92	-0.31
	500~500	non-divergent	8.37	2.93	1.48	-8.37	-2.93	-1.48
		divergent	15.23	5.76	2.55	-15.23	-5.76	-2.55

that divergence effect reduces the phase speeds of continental shelf waves.

If sea level fluctuations are set to zero at the shelf break as in the case (A), the 1st mode has Kelvin wave characteristics only when the shelf width is sufficiently large. However, if sea level fluctuations are allowed at offshore end of the shelf as in the cases (B) and (C), Kelvin waves are always present, irrespective of the cross-shelf dimension.

Fig. 5 shows the phase speeds of the first 3 continental shelf wave modes in the 400~80*km* double shelf case as shown in the section B of Fig. 1. Divergence effect is included, so that there are Kelvin wave modes as the 1st modes(the phase speeds of Kelvin wave modes will be mentioned later in Fig. 8.). The panels (A) and (B) in Figs. 5~9 are for the waves propagating northward along shelf 2 and southward along shelf 1, respectively. The magnitude of phase speed of the waves propagating southward is much more greater than that of the waves propagating northward, because of the wider shelf width. In Fig. 6, (a) is the same as in Fig. 5 but (b) is for a non-divergent case over the same double shelf. Compared to a non-divergent case, the phase speeds of continental shelf waves are reduced by divergence effects. The rate of reductions is greater in lower mode, up to about 35% in the first mode of continental shelf waves propagating southward.

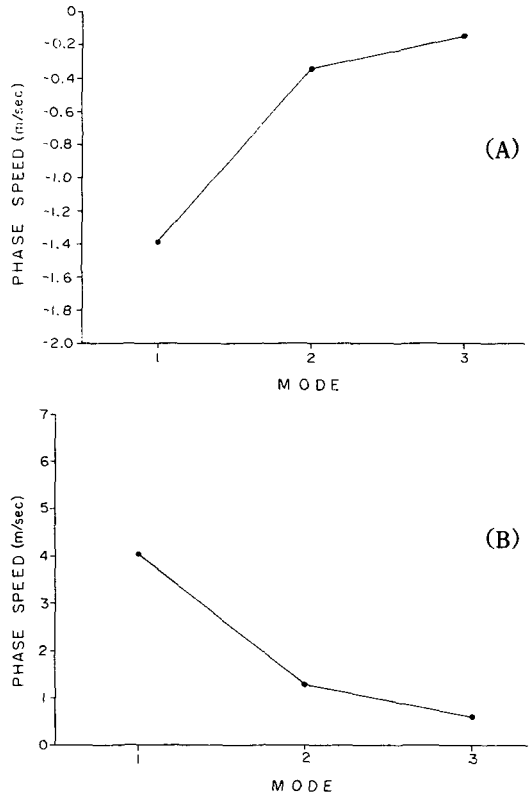

Fig. 5. Phase speeds of the first 3 continental shelf wave modes over a 400~80*km* double shelf for divergent case. Panels (A) and (B) are of the waves propagating northward along the shelf 2 and southward along the shelf 1, respectively. Phase speeds of Kelvin waves are shown in Fig. 8.

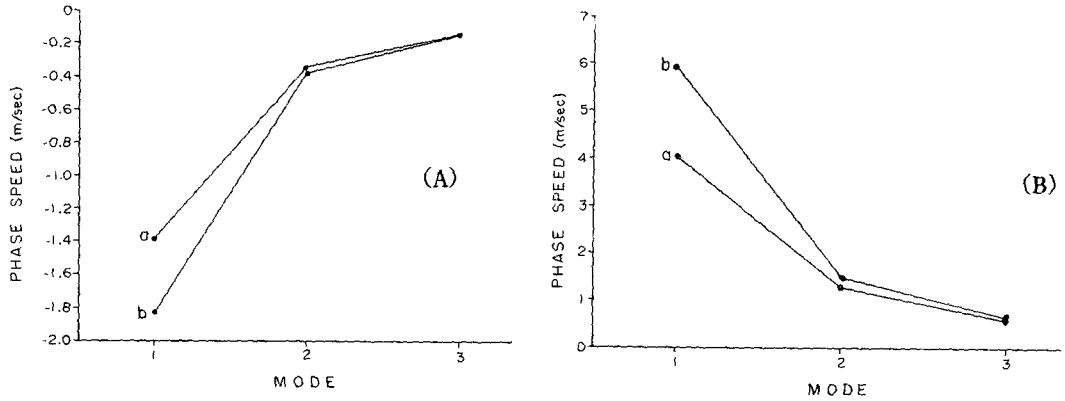

Fig. 6. Phase speeds of the first 3 continental shelf wave modes over a 400~80*km* double shelf for (a) divergent case and (b) non-divergent case. Panels (A) and (B) are of the waves propagating northward along the shelf 2 and southward along the shelf 1, respectively.

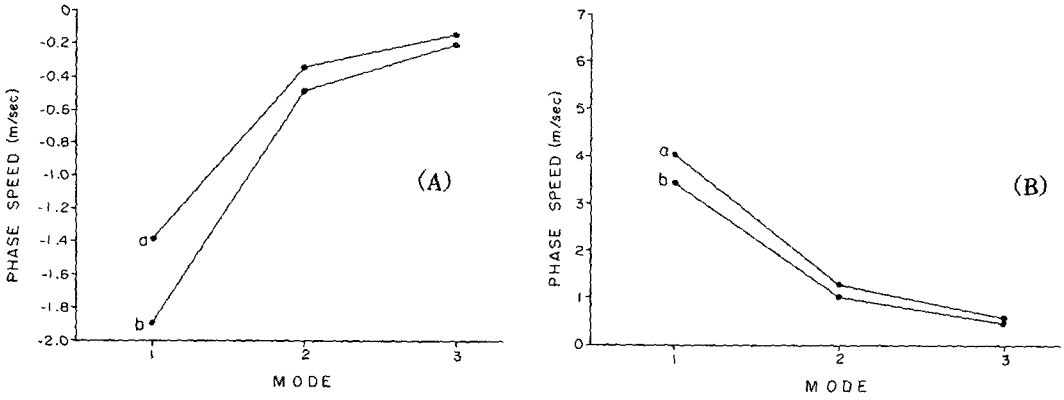

Fig. 7. Phase speeds of the first 3 continental shelf wave modes over (a) a 400~80*km* double shelf and (b) 300~120*km* double shelf for divergent case. Panels (A) and (B) are of the waves propagating northward along the shelf 2 and southward along the shelf 1, respectively.

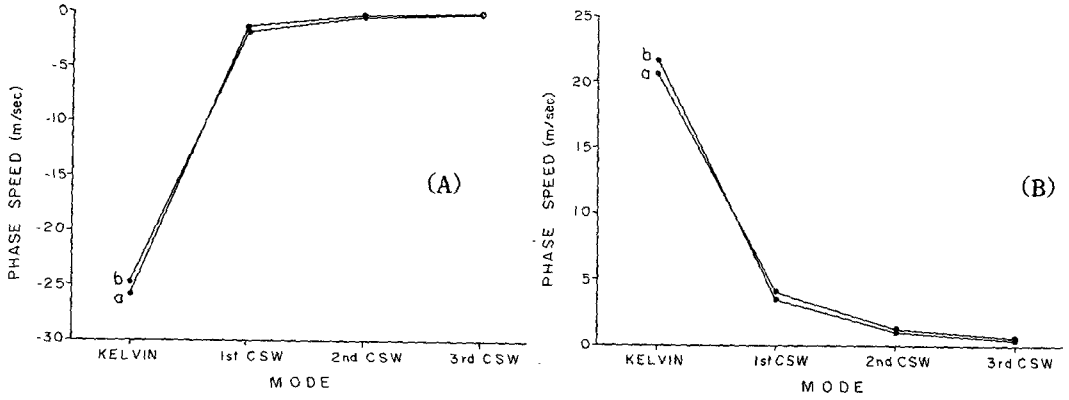

Fig. 8. Phase speeds of the Kelvin wave modes and the first 3 continental shelf wave modes over (a) a 400~80*km* double shelf and (b) 300~120*km* double shelf for divergent case. Panels (A) and (B) are of the waves propagating northward along the shelf 2 and southward along the shelf 1, respectively.

The phase speeds of continental shelf waves are also dependent on the coupled shelf widths in a double shelf. To see the variations of phase speeds by coupled shelf widths, two sections across the Yellow Sea as shown in Fig. 1 are selected. The shelf widths used in Fig. 7 are 400~80*km* for (a), as in Fig. 5, and 300~120*km* for (b). The phase speed of the continental shelf waves get larger for the waves propagating northward and smaller for the waves propagating southward. On the other hand, the phase speeds of Kelvin waves are affected only a little and even reversely by shelf width. The Kelvin waves are shown in Fig. 8, which is the same situation as Fig. 7. Phase speed of Kelvin wave is rather faster with smaller shelf width and hardly vary with the variation of shelf width.

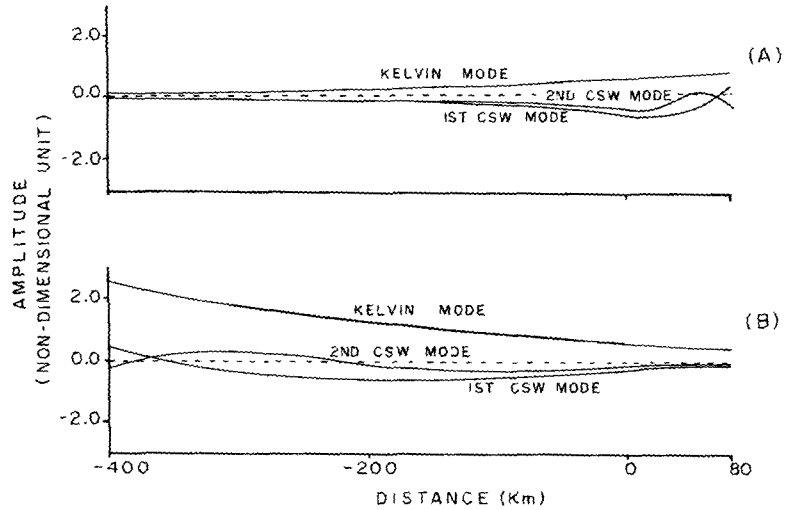

Fig. 9. The cross-shelf amplitudes of eigenfunction of the first 3 modes (Kelvin wave mode and the first 2 continental shelf wave modes) over a 400~80*km* double shelf for divergent case. Panels (A) and (B) are of the waves propagating northward along the shelf 2 and southward along the shelf 1, respectively.

Eigenfunctions and their Orthogonality

The eigenfunctions for the double shelf are as follows:

$$F=\begin{cases} F_1 & \text{in the shelf 1} \\ F_2 & \text{in the shelf 2} \end{cases}$$

$$F_1=\begin{cases} A\dfrac{u_2}{a_2T_1}[J_0(2a_2)Y_1(2a_2)-J_1(2a_2)Y_0(2a_2)] \\ \quad\times\left[-G_{12}J_0[2\{u_1(x+L_1)\}^{1/2}]+ G_{11}Y_0[2\{u_1(x+L_1)\}^{1/2}]\right] & \text{for } g\beta/f<c<0 \\ A\left[J_0[2\{u_1(x+L_1)\}^{1/2}]- (T_4/T_3)\cdot Y_0[2\{u_1(x+L_1)\}^{1/2}]\right] & \text{for } g\alpha/f>c>0 \end{cases} \quad (21\text{-}1)$$

$$F_2=\begin{cases} A\left[J_0[2\{u_2(x-L_2)\}^{1/2}]- (T_2/T_1)\cdot Y_0[2\{u_2(x-L_2)\}^{1/2}]\right] & \text{for } g\beta/f<c<0 \\ A\dfrac{u_1}{a_1T_3}[J_0(2a_1)Y_1(2a_1)-J_1(2a_1)Y_0(2a_1)] \\ \quad\times\left[-G_{22}J_0[2\{u_2(x-L_2)\}^{1/2}]+ G_{21}Y_0[2\{u_2(x-L_2)\}^{1/2}]\right] & \text{for } g\alpha/f>c>0 \end{cases} \quad (21\text{-}2)$$

where A is a arbitrary constant and

$$G_{11}=\frac{f}{c}J_0(2b_1)-\frac{u_1}{b_1}J_1(2b_1)$$

$$G_{12}=\frac{f}{c}Y_0(2b_1)\ \frac{u_1}{b_1}Y_1(2b_1)$$

$$G_{21}=\frac{f}{c}J_0(2b_2)-\frac{u_2}{b_2}J_1(2b_2)$$

$$G_{22}=\frac{f}{c}Y_0(2b_2)-\frac{u_2}{b_2}Y_1(2b_2)$$

$$T_1=[\frac{u_1}{a_1}J_1(2a_1)Y_0(2a_2)-\frac{u_2}{a_2}J_0(2a_1)Y_1(2a_2)]G_{12}$$
$$-[\frac{u_1}{a_1}Y_1(2a_1)Y_0(2a_2)-\frac{u_2}{a_2}Y_0(2a_1)Y_1(2a_2)]G_{11}$$

$$T_2=[\frac{u_1}{a_1}J_1(2a_1)J_0(2a_2)-\frac{u_1}{a_1}J_0(2a_1)J_1(2a_2)]G_{12}$$
$$-[\frac{u_1}{a_1}Y_1(2a_1)J_0(2a_2)-\frac{u_1}{a_1}Y_0(2a_1)J_1(2a_2)]G_{11}$$

$$T_3=[-\frac{u_1}{a_1}Y_1(2a_1)J_0(2a_2)+\frac{u_1}{a_1}Y_0(2a_1)J_1(2a_2)]G_{22}$$
$$-[-\frac{u_1}{a_1}Y_1(2a_1)Y_0(2a_2)+\frac{u_1}{a_1}Y_0(2a_1)Y_1(2a_2)]G_{21}$$

$$T_4=[-\frac{u_1}{a_1}J_1(2a_1)J_0(2a_2)+\frac{u_1}{a_1}J_0(2a_1)J_1(2a_2)]G_{22}$$
$$-[-\frac{u_1}{a_1}J_1(2a_1)Y_0(2a_2)+\frac{u_1}{a_1}J_0(2a_1)Y_1(2a_2)]G_{21}$$

Fig. 9 shows the amplitudes of the first 3 eifenfunctions across the shelf: (A) for $g\beta/f<c<0$ and (B) for $g\alpha/f>c>0$. Thus the sets of waves in Fig. 9 (A) and (B) propagate northward(into paper) along shelf 2 and southward(out of paper) along shelf 1, respectively. The 1st eigenfunctions are Kelvin wave. They have their maximum amplitudes at coast and decay exponentially across the whole shelf, without any node. They appear only when horizontal divergence is allowed. The rest eigenfunctions are continental shelf waves. They oscillate over one shelf and extend in an exponential decay over the other shelf. The 2nd modes are the 1st modes of continental shelf waves and have 1 node across the shelf. 3rd modes are the 2nd modes of continental shelf waves and have 2 node across the shelf, and so on.

Next the orthogonality of eigenfunctions should be proved for eigenfunction expansion.

Upon substituting for the pressure, $p=\sum_{n=-\infty}^{\infty}F_n(x)\phi_n(y+c_nt)$, the governing equation and boundary conditions for a double shelf topography are as follows:

$$[\alpha(x+L_1)F_{1n}']'+[-\ell^2\alpha(x+L_1)+f\frac{\alpha}{c_n}+\frac{\omega^2-f^2}{g}]F_{1n}=0$$
$$-L_1<x<0 \qquad (22\text{-}1)$$

$$[\beta(x-L_2)F_{2n}']'+[-\ell^2\beta(x-L_2)+f\frac{\beta}{c_n}+\frac{\omega^2-f^2}{g}]F_{2n}=0$$
$$0<x<L_2 \qquad (22\text{-}2)$$

$$F_{1n}'+\frac{f}{c_n}F_{1n}=0 \quad \text{at } x=-B_1 \qquad (23\text{-}1)$$
$$F_{1n}=F_{2n} \quad \text{at } x=0 \qquad (23\text{-}2)$$
$$F_{1n}'=F_{2n}' \quad \text{at } x=0 \qquad (23\text{-}3)$$
$$F_{2n}'+\frac{f}{c_n}F_{2n}=0 \quad \text{at } x=B_2 \qquad (23\text{-}4)$$

Multiplying the equations (22-1) & (22-2) by F_m and integrating them across the shelves yields

$$\int_{-B1}^{0}F_{1m}[\alpha(x+L_1)F_{1n}']'dx+\int_0^{B2}F_{2m}[\beta(x-L_2)F_{2n}']'dx$$
$$+[\frac{f\alpha}{c_n}+\frac{\omega^2-f^2}{g}]\int_{-B1}^{0}F_{1m}F_{1n}dx$$
$$+[\frac{f\beta}{c_n}+\frac{\omega^2-f^2}{g}]\int_0^{B2}F_{2m}F_{2n}dx$$
$$-\ell^2\alpha\int_{-B1}^{0}(x+L_1)F_{1m}F_{1n}dx-\ell^2\beta\int_0^{B2}(x-L_2)F_{1m}F_{1n}dx=0 \qquad (24)$$

By integration by parts and using the boundary conditions,

$$\alpha L_1F_{1m}(0)F_{1n}'(0)+\frac{f\alpha}{c_n}(-B_1+L_1)F_{1m}(-B_1)F_{1n}(-B_1)$$
$$+\beta L_2F_{2m}(0)F_{2n}'(0)+\frac{f\beta}{c_n}(-B_2+L_2)F_{2m}(-B_2)F_{1n}(-B_2)$$
$$-\int_{-B1}^{0}\alpha(x+L_1)F_{1m}'F_{1n}'dx-\int_0^{B2}\beta(x-L_2)F_{2m}'F_{2n}'dx$$
$$+[\frac{f\alpha}{c_n}+\frac{\omega^2-f^2}{g}]\int_{-B1}^{0}F_{1m}F_{1n}dx+[\frac{f\beta}{c_n}+\frac{\omega^2-f^2}{g}]$$
$$\int_0^{B2}F_{2m}F_{2n}dx-\ell^2\alpha\int_{-B1}^{0}(x+L_1)F_{1m}F_{1n}dx$$
$$-\ell^2\beta\int_0^{B2}(x-L_2)F_{1m}F_{1n}dx=0 \qquad (25)$$

Interchanging m and n and substracting them yields

$$\alpha L_1\cdot[F_{1m}(0)F_{1n}'(0)-F_{1m}'(0)F_{1n}(0)]$$
$$+\beta L_2\cdot[F_{2m}(0)F_{2n}'(0)-F_{2m}'(0)F_{3n}(0)]$$
$$+(\frac{f}{c_n}-\frac{f}{c_m})\Big[\alpha\int_{-B1}^{0}F_{1m}F_{1n}dx+\beta\int_0^{B2}F_{2m}F_{2n}dx$$
$$+\alpha(L_1-B_1)F_{1m}(-B_1)F_{1n}(-B_1)$$
$$+\beta(L_2-L_m)F_{2m}(B_2)F_{2n}(B_2)\Big]=0 \qquad (26)$$

The first two terms are zero by the boundary conditions. Therefore, when m is not n,

$$\alpha\int_{-B1}^{0}F_{1m}F_{1n}dx+\beta\int_0^{B2}F_{2m}F_{2n}dx-HF_mF_n\Big|_{-B1}^{B2}=0 \qquad (27)$$

To see if (27) does not hold when m=n, suppose to the contrary that

$$\alpha\int_{-B1}^{0} F_{1n}^2 dx+\beta\int_{0}^{B2} F_{2n}^2 dx-HF_n^2\Big|_{-B1}^{B2}=0 \qquad (28)$$

Multiplying (22-1) by F_{1n} and (22-2) by F_{2n} and integrating them across the shelf yields the following equation by the relation (28)

$$\int_{-B1}^{0} F_{1n}\cdot[\alpha(x+L_1)F_{1n}']'dx$$
$$+\int_{0}^{B2} F_{2n}\cdot[\beta(x-L_2)F_{2n}']'dx$$
$$-\frac{f^2}{g}\int_{-B1}^{B2} F_n^2 dx+\frac{f}{c_n}HF_n^2\Big|_{-B1}^{B2}=0$$

Integrating by parts and using the boundary conditions (23) leads us to

$$\int_{-B1}^{B2}[HF_n'^2 dx+\frac{f^2}{g}F_n^2]dx=0 \qquad (29)$$

Since the integrand $HF_n'^2 dx+\frac{f^2}{g}F_n^2$ is always positive, the assumption (28) creats a contradiction. Therefore, the assumption (28) does not hold when m=n. This leads us, with (27), to the following orthogonality condition.

$$\frac{\alpha\int_{-B1}^{0} F_{1m}F_{1n}dx+\beta\int_{0}^{B2} F_{2m}F_{2n}dx-HF_mF_n\Big|_{-B1}^{B2}}{\alpha\int_{-B1}^{0} F_{1n}^2 dx+\beta\int_{0}^{B2} F_{2n}^2 dx-HF_n^2\Big|_{-B1}^{B2}}=\delta_{mn} \qquad (30)$$

This proves that the eigenfunctions of coastally trapped wave over a double shelf are also orthogonal. From the orthogonality of eigenfunction, the method of eigenfunction expansion is possible for the forced problem. (The frictional eigenfunctions are not proved to be orthogonal, which is a difficulty in using the frictional eigenfunctions)

Discussion and Conclusion

For a single shelf adjacent to deep open ocean, the divergence effect might not be important. It depends on what kind of phenomenon we are looking at. For wind driven coastal motions, the divergence effect becomes important only when the shelf width is comparable to the Rossby defromation radius. However, for a double shelf, which allows sea level fluctuations at any place across channel, it is always important.

The divergence effect adds Kelvin wave to the solution of coastally trapped waves. As over a flat bottom, the amplitude of Kelvin wave has its maximum and decay exponentially away from coast. It has no node across the shelf. Its phase speed is modified by bottom slope, but essentially comparable to that of gravity wave. As a shelf is wider, the averaged depth is shallower, and therefore the phase speed of Kelvin wave is slower. This makes that the phase speed of Kelvin wave vary inversely with shelf width. On the other hand, phase speed of continental shelf waves is propotional to shelf width.

As for non-divergence case, there are also two sets of waves for divergence case. Each set include one Kelvin mode and infinite modes of continental shelf waves. The phase speeds of one set are positive and those of the other set are negative. The phase speeds of the Kelvin waves are much faster than that those of the continental shelf waves. The phase speeds of the shelf waves are slower for the higher mode. Thus, the 1st modes, which have the maximum phase speeds, are the Kelvin waves, and the 2nd modes are the 1st modes of continental shelf waves, and so on. The nth modes have n-1 nodes across the shelf. All the waves propagate with shallow waters to the right in Northern Hemisphere.

The two sets of waves are independent if two shelves are apart sufficiently and dependent on the geometry of both shelves if two shelves are close enough. The frictionless eigenfunctions of coastally trapped waves over a double shelf are proved to be orthogonal. It makes the method of eigenfunction expansion to be possible for the forced problem.

The dispersion relation is extended to high-frequency and short waves. Even for the extended case, the basic characteristics are preserved. The dispersion relation covers some limiting cases, such as low-frequency and long wave case. The extension is necessary for studies of reflection and scattering, etc.. The practical computations, however, are not inaccurate yet since confluent hypergeometric function is not fully developed.

References

Brink, K. H. 1983. Low-frequency free wave and wind-driven motions over a submarine bank. J. Phys. Oceanogr., 13, 103~116.

Brink, K. H. and J. S. Allen. 1978. On the effect of bottom friction on barotropic motion over the continental shelf. J. Phys. Oceanogr., 8, 919~922.

Buchwald, V. T. and J. K. Adams. 1968. The propagation of continental shelf waves. Proc. Roy. Soc. London, A305, 235~250.

Clarke, A. J. and S. Van Gorder. 1986. A method for estimating wind-driven frictional time-dependent, stratified shelf and slope water flow. J. Phys. Oceanogr., 16, 1013~1028.

Gill, A. E. and E. H. Schumann. 1974. The generation of long shelf waves by the wind. J. Phys. Oceanogr., 4, 83~90.

Hsueh, Y. and I. C. Pang. 1989. Coastally trapped long waves in the Yellow Sea. J. Phys. Oceanogr., 19, 5, 612~625.

Hsueh, Y. and R. D. Romea. 1983. Wintertime winds and coastal sea-level fluctuations in the Northeast China Sea. Part 1: Observations. J. Phys. Oceanogr., 13, 2091~2106.

Huthnance, J. M. 1975. On trapped waves over a continental shelf. J. Fluid Mech., 67, 689~704.

Huthnance, J. M. 1978. On coastal trapped waves: Analysis calculation by inverse iteration. J. Phys. Oceanogr., 8, 74~92.

LeBlond, P. H. and L. A. Mysak. 1978. Waves in the Oceans. Elsevier, 602pp.

Louis, J. P. 1978. Low-frequency edge waves over a trench-ridge topography adjoining a straight coastline. Geophys. Astrophys. Fluid Mech., 55, 113~127.

Mitchum, G. T. and A. J. Clarke. 1986. The frictional nearshore response to forcing by synoptic scale winds. J. Phys. Oceanogr., 16, 934~946.

Mysak, L. A. and P. H. LeBlond and W. J. Emery. 1979. Trench waves. J. Phys. Oceanogr., 9, 1001~1013.

Mysak, L. A. 1980. Recent advences in shelf wave dynamics. Rev. Geophys. Space Phys., 18, 211~241.

Mysak, L. A. and A. J. Willmott. 1981. Forced trench waves. J. Phys. Oceanogr., 11, 1481~1502.

Pang, I. C. 1987. Theory of coastally trapped waves and its application to the Yellow Sea. Ph. D. Dissertation, Florida State University, 128pp.

Pang, I. C. 1991. Coastally trapped waves over a double shelf topography (I): Free waves with exponential topography. Bull. Korean Fisher. Soc., 24(6), 428~436.

Received July 25, 1992
Accepted November 3, 1992

양향성 대륙붕의 대륙붕파 (II): 선형함수적 해저지형에서의 자유파

방 익 찬
제주대학교 해양학과

황해에서와 같은 선형의 양향성 대륙붕 해저 지형에서 저주파의 분산관계가 단주기·단파까지 포함하는 장주기·장파 경우에 대해 유도되었다. 선형의 양향성 대륙붕에서 장주기·장파일 경우 Bessel 방정식이 유도되는데 비해 일반적인 경우에는 Kummer 방정식이 유도된다. Kummer 방정식의 해로 유도되는 confluent Hypergeometric 함수는 극한 경우에 여러 형태로 바뀐다.

단일한 대륙붕에서는 해안선과 수직한 방향의 대륙붕 규모가 Rossby deformation radius에 비해 많이 작을 때는 수평흐름의 수렴·발산효과가 무시되지만 양향성 대륙붕에서는 수평흐름의 수렴·발산효과가 해안선과 수직한 방향의 대륙붕규모가 관계없이 파동역학에 결정적으로 중요하다. 수렴·발산효과는 Kelvin 파를 포함시키며 대륙붕파의 파속을 감소시킨다. 끝으로 양향성 대륙붕의 비마찰 eigenfunction들의 직교가 증명되었다.